Proteomic Analysis of Detergent-resistant Membrane Microdomains in Trophozoite Blood Stage of the Human Malaria Parasite *Plasmodium falciparum**[S]

Xue Yan Yam‡§¶, Cecilia Birago§‖, Federica Fratini‖, Francesco Di Girolamo‖, Carla Raggi‡‡, Massimo Sargiacomo‡‡, Angela Bachi§§, Laurence Berry‡, Gamou Fall‡, Chiara Currà‖, Elisabetta Pizzi‖, Catherine Braun Breton‡, and Marta Ponzi‖¶¶**

Intracellular pathogens contribute to a significant proportion of infectious diseases worldwide. The successful strategy of evading the immune system by hiding inside host cells is common to all the microorganism classes, which exploit membrane microdomains, enriched in cholesterol and sphingolipids, to invade and colonize the host cell. These assemblies, with distinct biochemical properties, can be isolated by means of flotation in sucrose density gradient centrifugation because they are insoluble in nonionic detergents at low temperature. We analyzed the protein and lipid contents of detergent-resistant membranes from erythrocytes infected by *Plasmodium falciparum*, the most deadly human malaria parasite. Proteins associated with membrane microdomains of trophic parasite blood stages (trophozoites) include an abundance of chaperones, molecules involved in vesicular trafficking, and enzymes implicated in host hemoglobin degradation. About 60% of the identified proteins contain a predicted localization signal suggesting a role of membrane microdomains in protein sorting/trafficking.

To validate our proteomic data, we raised antibodies against six *Plasmodium* proteins not characterized previously. All the selected candidates were recovered in floating low-density fractions after density gradient centrifugation. The analyzed proteins localized either to internal organelles, such as the mitochondrion and the endoplasmic reticulum, or to exported membrane structures, the parasitophorous vacuole membrane and Maurer's clefts, implicated in targeting parasite proteins to the host erythrocyte cytosol or surface. The relative abundance of cholesterol and phospholipid species varies in gradient fractions containing detergent-resistant membranes, suggesting heterogeneity in the lipid composition of the isolated microdomain population. This study is the first report showing the presence of cholesterol-rich microdomains with distinct properties and subcellular localization in trophic stages of *Plasmodium falciparum*. ***Molecular & Cellular Proteomics 12: 10.1074/mcp.M113.029272, 3948–3961, 2013.***

Plasmodium falciparum, the most deadly agent of human malaria, caused around 216 million infections and 655,000 deaths in 2010. The complex parasite life cycle involves the development in a mosquito vector of the *Anopheles genus* and eventual migration to a human host. In this host, asymptomatic multiplication in the liver cells is followed by parasite release into the bloodstream and erythrocyte invasion. Inside the erythrocytes, parasites grow (trophozoite stage) and multiply asexually (schizont stage), developing into highly specialized invasive forms (merozoites). A fraction of parasites differentiate into gametocytes, the gamete precursors necessary to complete the transmission cycle. Parasite blood stages, responsible for malaria pathogenesis and transmission, actively remodel the host erythrocyte, generating novel membrane compartments to sustain the export and sorting of proteins to the host cell cytosol, membrane skeleton, and plasma membrane. The parasitophorous vacuole membrane (PVM),[1] which surrounds the parasite throughout the erythrocytic cycle, is the site where exported proteins are translocated into the erythrocyte cytosol (1, 2). Membrane-bound structures of parasite origin, the so-called Maurer's clefts (MCs) (3, 4), form functionally independent compartments at

From the ‡University Montpellier II, CNRS UMR 5235, 34095 Montpellier, Cedex 5, France; ‖Dipartimento di Malattie Infettive Parassitarie ed Immunomediate, Istituto Superiore di Sanità, Viale Regina Elena 299, 00161, Rome, Italy; ‡‡Dipartimento di Ematologia, Oncologia e Medicina Molecolare, Istituto Superiore di Sanità, Viale Regina Elena 299, 00161, Rome, Italy; §§Dibit-San Raffaele Scientific Institute, 20123 Milano, Italy

Received March 15, 2013, and in revised form, August 29, 2013
Published, MCP Papers in Press, September 17, 2013, DOI 10.1074/mcp.M113.029272

[1] The abbreviations used are: DRM, detergent-resistant membrane; ER, endoplasmic reticulum; GPI, glycosylphosphatidyl inositol; iRBC, infected red blood cell; MC, Maurer's cleft; PBS, phosphate-buffered saline; PM, plasmepsin; PVM, parasitophorous vacuole membrane; RBC, red blood cell; SP, signal peptide; TM, transmembrane domain.

the red blood cell (RBC) periphery and mediate the sorting/assembly of virulence factors en route to the host cell surface (5). In addition, populations of different vesicles (25 and 80 nm) were identified in the RBC cytosol, suggesting the presence of vesicular mediated trafficking for the delivery of cargo to different destinations (6).

Membranes are important sites for cellular signaling events, and many proteins with therapeutic potential localize in these cellular compartments (7, 8). Membrane microdomains enriched in sphingolipids and cholesterol, also referred to as lipid rafts, have been extensively studied in different cell types and gained particular interest for their roles in infection and pathogenesis (8, 9). These assemblies are small and dynamic and can be stabilized to form larger microdomains implicated in a wide range of fundamental cellular processes, which vary depending on cell type (10). Sphingolipids exhibit strong lateral cohesion, generating tightly packed regions in the membrane bilayer, and cholesterol acts as a spacer present in both membrane leaflets generating stable, liquid-ordered phase domains in the membrane bilayer (11). Distinct biochemical properties render these membrane assemblies insoluble in nonionic detergents at low temperature, allowing for their enrichment as detergent-resistant membranes (DRMs). Proteins with DRM-raft affinity include glycosylphosphatidyl inositol (GPI)-anchored proteins and acylated, myristoylated, and palmitoylated proteins (11). DRM rafts also restrict free diffusion of membrane proteins, thereby directing the trafficking of proteins and lipids to and from cellular compartments. Because of their endocytic and receptor clustering capacity, an increasing number of pathogens, including *Plasmodium falciparum*, utilize them when interacting with their target cells for invasion (9, 12).

Even though cholesterol-rich membrane microdomains are implicated in fundamental processes in the parasite life cycle, *Plasmodium* is unable to synthesize sterols and depends entirely on hosts for its cholesterol supply. During merozoite invasion, lipid and protein components of the erythrocyte rafts are selectively recruited and incorporated into the nascent PVM (13, 14). *Plasmodium* liver stages utilize cholesterol internalized by low-density lipoprotein and synthesized by hepatocytes (15).

To shed light on the organization and dynamics of these assemblies during parasite development inside the infected cell, we identified and validated the DRM-raft proteome of the *P. falciparum* trophozoite/early schizont. Detected proteins only partially overlap with DRM components of the *P. falciparum* late schizonts (16, 17) or the mixed blood stages of the rodent malaria agent *P. berghei* (18). Immunolocalization of selected DRM-associated proteins indicated that these assemblies may reside in both exported compartments (PVM, MCs) and intracellular membranes/organelles. The analysis of DRM lipids suggested that distinct microdomains exist in the infected erythrocyte that differ in their relative abundance of cholesterol and phospholipids.

EXPERIMENTAL PROCEDURES

Plasmodium falciparum in Vitro Culture—*P. falciparum* 3D7 strain was maintained in continuous *in vitro* culture (19) in the presence of human erythrocytes at 5% hematocrit in RMPI 1640 medium containing 25 mM Hepes, 0.5% AlbuMAX II, 200 μM hypoxanthine, and 20 μg/ml gentamycin and incubated at 37 °C in a tri-gas mix of 5% O_2, 5% CO_2, and 90% N_2.

Parasite Synchronization—The parasite culture pellet was incubated with five volumes of sterile pre-warmed 5% sorbitol at 37 °C for 10 min and then centrifuged at 2000 rpm for 5 min at room temperature. Sorbitol-treated parasites were washed once with culture medium and put back in culture. Enrichment of late trophozoites and schizonts was accomplished via gelatin flotation with either Plasmion (Laboratoire Fresenius Kabi, Sèvres, France) or Gelofusine. The parasite pellet was incubated with 1.4 volumes of prewarmed culture medium and 2.4 volumes of prewarmed Plasmion or Gelofusine for 30 min at 37 °C. The upper phase containing the enriched late-stage parasites was collected and centrifuged at 2000 rpm for 5 min. The parasite pellet was washed once to remove the Plasmion or Gelofusine.

Purification and Analysis of P. falciparum Trophozoite/Early Schizont DRMs—DRMs from Plasmion/Gelofusine-enriched erythrocytes infected with *P. falciparum* trophozoites/early schizonts were prepared as described elsewhere (18). All procedures were performed at 4 °C with the addition of protease mixture inhibitors and PhosStop phosphatase inhibitor (Roche). Infected erythrocytes were lysed in 0.15 M NH_4Cl, 0.01 M $KHCO_3$, 1 mM EDTA. The parasite pellet (2×10^8 parasites) was suspended in 0.75 ml of MES-buffered saline (25 mM MES, pH 6.5, 0.15 M NaCl) containing 1% Triton X-100 (v/v) and homogenized with a Potter-Elvehjem glass homogenizer. Parasite extract was adjusted to 40% sucrose by the addition of 0.75 ml of 80% sucrose, prepared in MES-buffered saline, placed at the bottom of an ultracentrifuge tube (4.5 ml, 13 × 15 mm, Beckman) and overlaid with 1.5 ml of 30% sucrose and 1.5 ml of 5% sucrose. Samples were centrifuged (45,000 rpm for 16 h at 4 °C) in an SW60Ti rotor (Beckman Instruments). 375-μl fractions were collected from the top of each gradient. DRMs containing flotillin, a lipid raft marker, appeared as an opaque band at 10% to 20% sucrose (fractions 4 and 5). For proteomic analyses, these fractions were pooled, diluted 1:5, and centrifuged at 30,000 × *g* for 30 min at 4 °C. The membrane pellet was subjected to a second sucrose gradient in order to minimize the presence of spurious contaminants. After centrifugation, proteins contained in fractions 4 and 5 were identified via mass spectrometry (see below).

Expression and Purification of Recombinant Proteins—Coding regions of the selected genes were amplified and cloned in frame with the glutathione *S*-transferase (GST) tag of the pGEX vector. Recombinant proteins were expressed in C41 competent cells. Soluble GST fusions were purified on glutathione-Sepharose beads. Insoluble GST fusions were subjected to SDS-PAGE, and gel slices containing Coomassie Blue–stained polypeptides were electro-eluted using a Bio-Trap electro-elution device (Schleicher & Schuell, Dassel, Germany). Primers used for PCR amplification and gel-separated recombinant proteins are shown in the supplemental "Materials and Methods" section.

Antibodies—Antibodies raised against DRM-associated proteins were induced via subcutaneous immunization of 6- to 8-week-old BALB/c mice with 20 to 50 μg of purified protein (first injection in Freund's complete adjuvant; two further injections, performed at 2-week intervals, in Freund's incomplete adjuvant). Mice were bled 1 week after the third immunization. Sources of other antibodies used in this study and the dilutions adopted are detailed in the supplemental "Materials and Methods" section.

Indirect Immunofluorescence Assay—*P. falciparum*–infected RBCs (iRBCs) were fixed in 4% paraformaldehyde with 0.0075% glutaraldehyde (EMS Science, Hatfield, PA) in phosphate-buffered saline (PBS) overnight at 4 °C. The next steps were all conducted at room temperature. Fixed cells were washed in PBS, permeabilized with 0.1% Triton X-100 in PBS for 10 min, and treated with 0.1 M glycine in PBS for 10 min to block free reactive aldehyde groups. iRBCs were incubated in succession with 3% fetal calf serum (FCS) in PBS for 1 h and the primary antibody diluted with 3% FCS in PBS for 1 h. After several washes using 1% FCS in PBS, fixed cells were incubated for 1 h with the secondary antibody conjugated to Alexa 488 or 594 (molecular probe, 1:2000 dilution in 3% FCS in PBS) and washed again. Nuclei were stained with Hoechst 33342 (1:10,000 dilution in PBS). Samples were layered on poly-L lysine-coated immunofluorescence slides (Sigma P8920) and mounted with VECTASHIELD. Slides were viewed under a Zeiss Axioimager epifluorescence microscope (Axio Imager 2). When Z-stack acquisition was performed, images with a slice distance of 0.3 μM were presented. For mitochondria labeling, parasite cultures were incubated for 30 min with MitoTracker® probe (M7512, Invitrogen) at a final concentration of 20 nM in Hank's balanced salt solution. Samples were then washed once with Hank's balanced salt solution medium, fixed in 4% paraformaldehyde, 0.0075% glutaraldehyde in PBS overnight at 4 °C, and further processed as described above.

In-gel Tryptic Digestion—

Experiment A—DRM-raft proteins (fractions 4 and 5) were precipitated, solubilized in Laemmli sample buffer at 65 °C for 1 h, loaded on SDS-PAGE (homemade 5% stacking/12% resolving), and run just long enough to allow the protein marker (BenchMark™ Pre-Stained Protein Ladder, Invitrogen) to enter the resolving gel. After Coomassie staining (Novex, Colloidal Blue staining gel, Invitrogen), unseparated bands were excised and in-gel tryptic digestion was performed as described below. Supernatants were used directly for LC-MS/MS analysis.

Experiment B—Proteins contained in fractions 4 and 5 were separated on Invitrogen precast 4–20% Bis-Tris Gels and stained with Coomassie Colloidal Blue. After visualization, each sample lane was cut into sequential slices. Gel slices were destained in 50 mM NH_4CO_3/CH_3CN 1:1 and covered with acetonitrile until the gel pieces shrank. The acetonitrile was removed and the gel particles were dried by centrifugation under vacuum. Proteins were reduced (10 mM DTT, 25 mM NH_4CO_3) for 30 min at 56 °C, shrunk with acetonitrile, and alkylated (55 mM iodoacetamide, 25 mM NH_4CO_3) for 30 min in the dark at room temperature. Gel pieces were washed in 50 mM NH_4CO_3/CH_3CN 1:1 for 15 min and covered with acetonitrile until they shrank. Acetonitrile was removed and gel particles were dried by centrifugation under vacuum. In-gel digestion was performed by adding 12.5 ng/μl of trypsin (Promega) in 25 mM NH_4CO_3 at 37 °C overnight under stirring. Supernatants were directly used for mass spectrometry analysis.

Mass Spectrometry Analyses—

Experiment A: Nano-LC-MS/MS on an LTQ XL Ion Trap—Nano-RPLC was performed using a nano-HPLC 3000 Ultimate (Dionex, Sunnyvale, CA) connected online to an LTQ-XL linear ion trap (Thermo Fisher). Tryptic digests (20 μl) were first loaded on a C18 reversed-phase pre-column (300 μm inner diameter $\times$ 5 mm; 5-μm particle size; 100-Å pore size; LC Packings-Dionex) and washed by the loading pump at 20 μl/min with buffer A (5% CH_3CN, 0.1% HCOOH) for 5 min and then on a homemade 13 cm $\times$ 75 μm inner diameter Silica PicoTip (8 $\pm$ 1 μm) column (PicoTip Emitter, New Objective, Woburn, MA) packed with Magic C18AQ (5-μm particle size; 200-Å pore size; Michrom Bioresouces Inc., Auburn, CA) for chromatographic separations. Peptides were eluted at 0.3 μl/min along a 120-min linear gradient from 20% to 60% buffer B (95% CH_3CN, 0.1% HCOOH) and electro-sprayed directly into the mass spectrometer with a spray voltage of 1.60 to 1.65 kV and a capillary temperature of 180 °C. Data acquisition was performed in Top5 data-dependent mode to automatically switch between MS and MS^2. Full-scan MS parameter settings were as follows: automatic gain control value of 30,000 ions, maximum injection time of 50 ms, and *m/z* 400–2000 mass range. The five most intense ions were sequentially selected and fragmented in collision-induced dissociation mode with the following parameter settings: isolation width of 2.0, automatic gain control value of 10,000 ions, maximum injection time of 100 ms, *m/z* 50–2000 mass range, collision energy of 35%, minimum signal threshold of 200 counts, and wide band activation on. A dynamic exclusion of ions previously sequenced within 60 s was applied.

Experiment B: Nano-LC-MS/MS on Hybrid Quadrupole TOF-MS—Samples (5 μl) were mixed with an equal volume of 3% acetonitrile, 1% formic acid and analyzed via nano-LC electrospray ionization MS/MS. Chromatographic separations were carried out using a 75-μm inner diameter, 15-cm-long fused silica capillary column (LC Packings PepMap, 100 A). Nano-reversed-phase LC was performed using an Agilent 1100 system (Agilent Technologies, Santa Clara, CA). After sample injection, the column was washed for 5 min with 90% mobile phase A (2% CH_3CN, 0.1% HCOOH) and peptides eluted using a linear gradient from 10% to 90% mobile phase B (98% CH3CN, 0.1% HCOOH) over 75 min with a constant flow rate of 0.2 μl/min. The nano-reversed-phase LC column was coupled online to a hybrid quadrupole TOF mass spectrometer (API Q-STAR *pulsar*, PE SCIEX, Toronto, ON, Canada) using a nano-electrospray source (Proxeon Biosystems, Odense, Denmark) with an applied electrospray potential of 1800 V; the *m/z* range was 350–1400 for MS and 100–2000 for MS/MS. Spectra were recorded using external calibration. Raw MS/MS data were analyzed using Analyst QS 1.1 (Applied Biosystems, Darmstadt, Germany) as provided by the manufacturer and were reported as monoisotopic masses.

Spectra files from both experiments were analyzed by the Sequest search engine with Proteome Discoverer 1.4 (ThermoFisher) using a homemade database constructed with the Human UniProt–SwissProt database (released June 2012) and *P. falciparum* 3D7 (PlasmoDB 9.2, released November 2012) and containing a decoy database (150,994 total entries). Carbamidomethylation of cysteines was specified as a fixed modification, and the oxidation of methionine was set as a variable modification. The mass tolerance was set to 0.8 Da for precursor ions and 0.4 Da for fragment ions, and a maximum of two missed cleavages was allowed. The Percolator tool was used for peptide validation based on the q-value, and high confidence was chosen, corresponding to a false discovery rate of $\leq$1% on the peptide level. Proteins were identified with a minimum of two peptides (rank = 1) in both experiments.

Bioinformatics Analysis—A manually curated functional classification was performed on the basis of the Gene Ontology annotation available in PlasmoDB.

Gene expression profiling of the DRM-associated proteins was reconstructed from RNA sequencing data (20) available in PlasmoDB. For each of the six time points, rings, early trophozoites, late trophozoites, schizonts, early gametocytes of stage II, and late gametocytes of stage V were analyzed. RNA abundance values (x) were normalized according to

$$Z = \frac{(x - m)}{stdv} \quad \text{(Eq. 1)}$$

where m is the mean value and stdv is the standard deviation.

The self-organizing tree algorithm was used to group normalized gene expression profiles. The Pearson correlation coefficient was chosen as a metric, and the "max cycle" parameter was fixed at 7 to obtain six clusters.

Transmembrane helices were predicted using TMHMM 2.0. GPI-SOM was used to predict the GPI-anchor addition. plasmodium export element–containing *Plasmodium* exported proteins were predicted using dedicated software (21).

Lipid Extraction and Analysis—Trophozoite-infected RBCs (6×10^8) were purified and host cells were subjected to osmotic lysis. Recovered parasites were suspended in cold Triton, and Triton-insoluble material was fractionated by means of discontinuous sucrose gradient centrifugation (see the paragraph on parasite purification and analysis in the preceding section). Fractions 2–6 were diluted 1:5 and centrifuged at 30,000 $\times$ *g* for 30 min at 4 °C. Lipids were extracted from pellets using a chloroform:methanol (2:1, v/v) solution according to the procedure described by Folch *et al.* (22). Extracts were dried under nitrogen atmosphere and used for neutral lipid and phospholipid thin layer chromatography (TLC). TLC for neutral lipids was done by eluting lipid extract in a solution of hexane:diethylether: acetic acid (70:30:1, v/v). TLC for phospholipids was performed by running lipid extract in a chloroform:methanol:acetic acid:formic acid: H_2O (35:15:6:2:1, v/v) solution in order to separate sphingomyelin, phosphatidylcholine, and phosphatidylethanolamine. The spots were visualized via copper acid staining (3% w/v). The plate was heated for about 5 min at 180 °C, and the abundance of the different lipid classes in each fraction was estimated in comparison with lipid standards (Sigma-Aldrich Corporation, St. Louis, MO) using a GS-700 imaging densitometer (Bio-Rad).

RESULTS

DRM Proteome of P. falciparum Late Trophozoites/Early Schizonts—Trophozoite/early schizont-infected RBCs were purified from highly synchronous *P. falciparum* cultures. Intact parasites and associated membranous structures were recovered after osmotic lysis of the erythrocyte plasma membrane (18). DRM rafts were then isolated based on their resistance to Triton X-100 extraction at low temperature and their specific density in discontinuous sucrose gradients (18). DRM rafts, detected as an opaque band floating to the 5%-to-30% sucrose boundary (fractions 4 and 5), were collected and further purified through a second sucrose gradient to minimize the presence of spurious contaminants. In order to obtain a robust dataset, two entirely independent biological replicates were analyzed, and only the overlap between the identified proteomes was considered for further characterization. In experiment A, the peptide mixtures of fractions 4 and 5 were analyzed separately on a 2-hour-long gradient and subjected to MS/MS analysis on an LTQ XL Ion Trap. In this case we detected 158 parasite proteins matching the imposed criteria (false discovery rate of $\leq$1 and at least two peptides (rank 1) identified per protein). In experiment B, pooled DRM fractions 4 and 5 were precipitated and protein components were separated via one-dimensional SDS-PAGE. Coomassie Colloidal Blue–stained gel was cut into slices, trypsin digested, and subjected to MS/MS analysis on a hybrid quadrupole TOF mass spectrometer. Using this procedure, we identified 93 *Plasmodium* proteins that passed the imposed filters. The final compiled list (Table I) included 83 common proteins detected with false discovery rates of $\leq$1 and two peptides in both experiments and a conserved *Plasmodium* protein of unknown function (PF3D7_1013300), identified with four peptides in experiment A and one in experiment B. We included this protein because its presence in parasite DRMs was supported by data obtained previously in our laboratory (not shown). Various members of the MC-resident 2TM family were identified, but only PF3D7_0222100, detected in both experiments, is reported in Table I. The presence of microdomains in the MC membranes explains previous observations suggesting that the delivery of virulence factors from MCs to the RBC membrane involves cholesterol-rich microdomains (23).

To define cellular processes associated with trophozoite/early schizont DRM rafts, we assigned the identified *P. falciparum* proteins to functional categories based on the annotation available in PlasmoDB (Fig. 1).

As shown in Table I, 37 proteins identified in this study had already been reported in the DRM proteome of *P. falciparum* late schizonts (16). Among them, we found factors related to the host erythrocyte invasion, eight membrane transporters (PF3D7_0523000, PF3D7_0914700, PF3D7_1132800, PF3D7_1211900, PF3D7_1347200, PF3D7_1432100, PF3D7_1456800, PF3D7_0316600), three members of a small family of GPI-anchored proteins (P41 (PF3D7_0404900), Pf38 (PF3D7_0508000), and Pf12 (PF3D7_0612700)) characterized by six cysteines (cys) conserved in their position (24), two additional cysteine-rich proteins (Pf 92 (PF3D7_1364100) and Pf113 (PF3D7_1420700)) that do not exhibit structural features distinctive of the 6-cys family, and components of the PVM-resident translocon machinery (PF3D7_1436300, PF3D7_1471100, PF3D7_1116800), implicated in the export of parasite proteins across the PVM (2). Thirteen other proteins had been identified previously in the DRM proteome of *P. berghei* mixed blood stages, and 34 novel proteins were identified in this study. Based on this comparative analysis, 47 DRM-associated proteins detected in this study, but not in the DRM proteome of *P. falciparum* late schizonts, might be considered potential trophozoite/early schizont-specific candidates. They include an abundance of molecular chaperones, five RAB GTPases, and a vesicle-associated membrane protein (PF3D7_1439800). This strongly suggests that DRMs may act as regulators of protein sorting and trafficking during parasite growth and host cell remodeling.

Notably, the four plasmepsins (PMs) encoded by the *P. falciparum* genome, PM I, PM 2, PM III (or HAP), and PM IV, partition into DRMs during trophozoite development. These aspartic proteases are involved in the catabolism of host hemoglobin internalized by the parasite during intraerythrocytic development (25).

Mass spectrometry data available in PlasmoDB indicated that the majority of proteins detected in this study are expressed in both asexual and sexual blood stages of *P. falciparum*, with the exception of eight proteins identified only in asexual stages. They include two members of the 6-cys family (PF3D7_1364100, PF3D7_0404900); the merozoite surface protein MSP7 (PF3D7_1335100); a nucleoside transporter

TABLE I
DRM-raft proteome of P. falciparum trophozoite/early schizonts

Accession	Description	Experiment A			Experiment B			MW (kDa)	SP	TM	GPI	*Pf* schizont DRMs	*Pb* blood stage DRMs
		Score	Coverage	Peptides	Score	Coverage	Peptides						
PF3D7_0207600	Serine repeat antigen 5 (SERA5)	34.34	5.02	4	5.47	2.71	2	111.7	y			y	
PF3D7_0222100	Pfmc-2TM Maurer's cleft two-transmembrane protein (MC-2TM)	27.15	10.04	2	10.01	9.17	2	27.0	y	y			
PF3D7_0316600	Formate-nitrite transporter, putative	87.22	10.68	3	10.19	6.47	2	34.4		y		y	
PF3D7_0318100	Band 7–related protein	10.78	7.75	2	4.55	5.35	2	43.1					
PF3D7_0404900	6-cysteine protein (P41)	28.81	21.16	5	43.96	28.04	8	43.1	y			y	y
PF3D7_0416800	Small GTP-binding protein sar1 (SAR1)	13.25	25.00	3	6.28	12.50	2	22.0					
PF3D7_0501500	Rhoptry-associated protein 3 (RAP3)	39.66	16.50	5	23.33	19.50	8	47.0	y			y	y
PF3D7_0501600	Rhoptry-associated protein 2 (RAP2)	74.16	28.14	9	38.89	30.90	10	46.7	y			y	
PF3D7_0508000	6-cysteine protein (P38)	79.71	10.32	3	31.17	32.66	8	40.6	y		y	y	
PF3D7_0512600	Rab GTPase 1b (Rab1b)	293.68	25.50	4	8.21	10.50	2	22.9					y
PF3D7_0523000	Multidrug resistance protein (MDR1)	126.75	14.52	13	4.50	1.34	2	162.1		y		y	
PF3D7_0524000	Karyopherin beta (KASbeta)	25.49	4.01	3	11.67	4.27	4	127.3					
PF3D7_0532100	Early transcribed membrane protein 5 (ETRAMP5)	45.27	20.44	2	37.52	20.44	2	19.0	y	y			
PF3D7_0606800	Probable protein, unknown function	178.40	36.45	8	38.51	34.78	9	34.5	y				
PF3D7_0608800	Ornithine aminotransferase (OAT)	13.25	5.56	2	26.08	21.26	8	46.0					
PF3D7_0612700	6-cysteine protein (P12)	91.51	36.89	9	39.70	23.34	7	39.4	y		y	y	y
PF3D7_0626800	Pyruvate kinase (PyrK)	50.18	17.61	5	15.44	8.41	4	55.6					
PF3D7_0707300	Rhoptry-associated membrane antigen (RAMA)	25.65	6.04	3	32.60	7.20	4	103.6	y		y	y	
PF3D7_0708400	Heat shock protein 90 (HSP90)	151.39	26.71	15	29.53	10.47	7	86.1					y
PF3D7_0713700	Conserved *Plasmodium* protein, unknown function	42.82	28.71	4	6.17	11.00	2	24.4	y	y			
PF3D7_0721100	Conserved *Plasmodium* protein, unknown function	51.90	29.51	5	8.97	13.11	3	29.2	y			y	
PF3D7_0807300	Rab GTPase 18 (RAB18)	36.04	24.88	4	5.01	10.45	2	23.1					
PF3D7_0814200	DNA/RNA-binding protein Alba 1 (ALBA1)	40.69	17.74	3	4.11	8.06	2	27.2					
PF3D7_0818200	14–3-3 protein, putative	89.54	24.81	6	8.72	9.92	2	30.2					y
PF3D7_0818900	Heat shock protein 70 (Hsp70)	284.04	33.38	17	125.38	38.85	22	73.9				y	y
PF3D7_0819600	Conserved *Plasmodium* protein, unknown function	44.81	31.05	5	12.71	20.22	5	32.1				y	
PF3D7_0827900	Protein disulfide isomerase (PDI8)	157.07	37.27	12	15.86	13.25	5	55.5	y				y
PF3D7_0831700	Heat shock protein 70, putative (HSP70-x)	85.47	15.46	8	41.36	11.34	7	75.0	y				
PF3D7_0903200	Rab GTPase 7 (Rab7)	198.53	62.14	8	23.86	35.44	6	23.8					y
PF3D7_0912400	Conserved *Plasmodium* protein, unknown function	91.96	20.63	7	11.53	14.35	5	52.7	y	y			
PF3D7_0914700	Transporter, putative	31.68	8.72	3	9.04	3.49	2	58.4		y		y	
PF3D7_0917900	Heat shock protein 70 (Hsp70–2)	355.91	32.67	18	70.08	34.97	18	72.3	y			y	y
PF3D7_0918000	Glideosome-associated protein 50, secreted acid phosphatase	142.29	31.06	8	23.13	19.19	6	44.6	y	y		y	
PF3D7_0922500	Phosphoglycerate kinase (PGK)	61.22	28.37	9	9.25	8.17	3	45.4					
PF3D7_0925900	Conserved *Plasmodium* protein, unknown function	177.79	18.43	3	17.05	23.04	4	24.7	y				
PF3D7_0929400	High molecular weight rhoptry protein 2 (RhopH2)	12.33	1.52	2	10.16	2.90	4	162.6	y			y	
PF3D7_0930300	Merozoite surface protein 1 (MSP1)	743.85	25.12	35	775.98	32.03	48	195.6	y		y	y	y
PF3D7_1008900	Adenylate kinase (AK1)	75.47	35.12	6	9.56	16.53	3	27.6					
PF3D7_1012400	Hypoxanthine-guanine phosphoribosyltransferase (HGPRT)	45.09	24.68	4	9.49	16.02	3	26.3					
PF3D7_1013300*	Conserved *Plasmodium* protein, unknown function	23.48	8.12	4	2.52	2.39	1	75.4	y	y			y
PF3D7_1015900	Enolase (ENO)	88.43	31.61	9	20.81	17.49	6	48.6					y
PF3D7_1020900	ADP-ribosylation factor (ARF1)	75.34	43.65	6	8.58	11.60	2	20.9					
PF3D7_1029600	Adenosine deaminase, putative	10.75	16.08	4	15.89	13.35	4	42.4					y
PF3D7_1104400	Conserved protein, unknown function	96.12	24.06	9	14.93	13.44	6	49.2	y				

TABLE I—*continued*

Accession	Description	Experiment A			Experiment B			MW (kDa)	SP	TM	GPI	*Pf* schizont DRMs	*Pb* blood stage DRMs
		Score	Coverage	Peptides	Score	Coverage	Peptides						
PF3D7_1105100	Histone H2B (H2B)	12.31	21.37	2	13.06	14.53	2	13.1					
PF3D7_1105400	40S ribosomal protein S4, putative	4.78	10.73	2	5.26	7.28	2	29.8				y	
PF3D7_1105800	Conserved *Plasmodium* protein, unknown function	81.68	19.17	4	7.81	13.16	3	30.6	y				
PF3D7_1115600	Peptidyl-prolyl cis-trans isomerase (CYP19B)	95.64	31.79	6	6.87	14.36	3	21.7	y				
PF3D7_1116800	Heat shock protein 101 (HSP101)	473.81	44.70	33	176.02	47.24	35	102.8	y			y	
PF3D7_1121600	Circumsporozoite-related antigen (EXP1)	24.54	17.90	3	26.52	17.28	3	17.3	y	y		y	y
PF3D7_1129000	Spermidine synthase (SpdSyn)	67.70	18.38	4	21.18	19.63	5	36.6					
PF3D7_1130200	60S ribosomal protein P0	24.36	15.82	3	5.36	8.86	3	34.9				y	
PF3D7_1132800	Aquaglyceroporin (AQP)	27.54	12.40	3	11.49	12.40	3	28.3	y	y		y	
PF3D7_1134000	Heat shock protein 70 (Hsp70–3)	103.95	18.40	9	28.85	18.25	9	73.3				y	
PF3D7_1144900	Rab GTPase 6 (RAB6)	145.39	27.54	5	23.95	30.43	7	23.6					y
PF3D7_1211900	Non-SERCA-type Ca2-transporting P-ATPase (ATP4)	32.39	6.65	6	4.97	1.27	2	140.2		y		y	
PF3D7_1212000	Glutathione peroxidase (Trx-G1)	15.12	14.63	2	14.99	12.68	3	23.9	y			y	
PF3D7_1222300	Endoplasmin homolog precursor, putative	203.97	24.73	15	26.46	10.11	7	95.0	y				y
PF3D7_1237700	Conserved *Plasmodium* membrane protein, unknown function	59.41	14.76	3	3.06	10.00	2	23.6		y		y	
PF3D7_1302800	40S ribosomal protein S7, putative	12.13	26.29	3	4.19	8.25	2	22.5				y	
PF3D7_1320600	Rab GTPase 11a (RAB11a)	43.71	18.52	3	21.92	40.28	8	24.7					
PF3D7_1335100	Merozoite surface protein 7 (MSP7)	107.27	22.79	7	23.61	21.08	5	41.3	y			y	y
PF3D7_1343000	Phosphoethanolamine N-methyltransferase (PMT)	55.48	53.76	10	14.04	12.78	3	31.0					
PF3D7_1344800	Aspartate carbamoyltransferase (atcasE)	74.44	20.27	6	17.36	17.07	6	43.2	y				
PF3D7_1347200	Nucleoside transporter 1 (NT1)	77.69	4.50	3	4.73	3.79	2	47.6		y		y	
PF3D7_1352500	Thioredoxin-related protein, putative	129.46	27.88	6	32.28	25.96	5	24.0	y	y			y
PF3D7_1357000	Elongation factor 1-alpha	314.87	40.63	12	38.67	25.73	9	48.9				y	y
PF3D7_1364100	Cysteine-rich surface protein (Pf92)	446.41	37.94	21	371.89	40.95	25	92.7	y		y	y	
PF3D7_1407800	Plasmepsin IV (PM4)	54.37	14.70	4	10.16	10.91	3	51.0		y			y
PF3D7_1407900	Plasmepsin I (PMI)	148.05	28.32	10	26.29	26.33	9	51.4		y			
PF3D7_1408000	Plasmepsin II	154.20	28.70	9	6.14	6.84	2	51.4		y			
PF3D7_1408100	Plasmepsin III, histo-aspartic protease (HAP)	215.96	33.48	10	24.30	17.96	7	51.7		y			
PF3D7_1410400	Rhoptry-associated protein 1 (RAP1)	160.60	25.19	13	88.22	26.21	16	90.0	y			y	y
PF3D7_1410700	Conserved *Plasmodium* protein, unknown function	70.47	34.13	9	6.26	9.28	3	39.8	y				
PF3D7_1420700	Surface protein, Pf113 (Pf113)	120.77	15.79	11	291.30	42.41	29	112.5	y		y	y	
PF3D7_1424100	60S ribosomal protein L5, putative	42.55	13.95	3	3.73	5.78	2	34.0					
PF3D7_1432100	Conserved protein, unknown function	67.09	15.92	4	11.82	11.42	3	33.2				y	
PF3D7_1436300	Translocon component PTEX150 (PTEX150)	201.41	19.54	15	125.59	13.70	11	112.3	y			y	
PF3D7_1439800	Vesicle-associated membrane protein, putative	27.58	30.29	5	3.27	12.03	2	27.7					
PF3D7_1439900	Triosephosphate isomerase (TIM)	14.26	20.97	3	5.76	12.10	3	27.9					y
PF3D7_1456800	V-type H( )-translocating pyrophosphatase, putative	142.77	21.06	12	29.48	9.48	6	76.4	y	y		y	
PF3D7_1462800	Glyceraldehyde-3-phosphate dehydrogenase (GAPDH)	78.15	47.48	10	50.23	38.87	10	36.6					
PF3D7_1468700	Eukaryotic initiation factor 4A (eIF4A)	48.03	19.10	4	5.20	5.78	2	45.3					
PF3D7_1471100	Exported protein 2 (EXP2)	421.56	35.54	13	211.64	32.40	10	33.4	y			y	y

Notes: DRM-associated proteins of *P. falciparum* trophozoites/early schizonts identified in two independent biological replicates (experiments A and B) with a false discovery rate of ≤1 and two peptides reported. PF3D7_1013300* (detected with four peptides in experiment A and one peptide in experiment B) was included in the list based on previous results. "Score," "coverage," and "peptides" (number of peptides identified) values are from Proteome Discoverer 1.4 software using the Sequest search engine. Localization signals are reported as annotated in PlasmoDB. SP, signal peptide; TM, transmembrane domain; GPI, glycosylphosphatidyl inositol anchor; Y, presence; *Pf* schizont DRMs, proteins detected in *P. falciparum* schizont DRMs as described (16); *Pb* blood stage DRMs, proteins detected in *P. berghei* mixed blood stage DRMs as described (18).

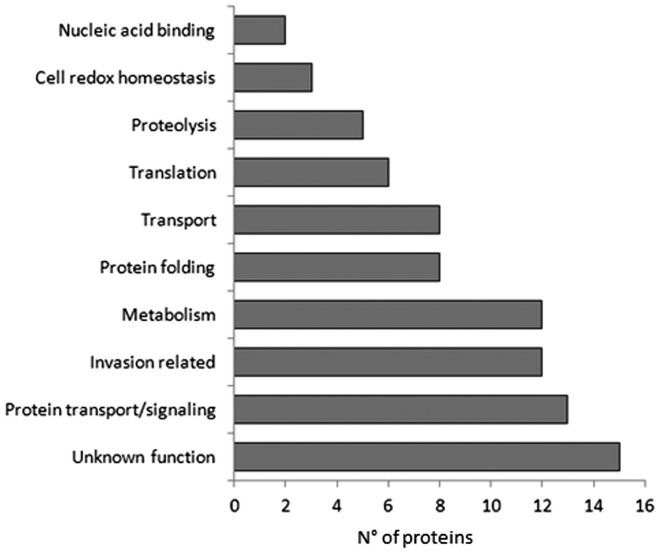

FIG. 1. **Major functional categories associated with DRMs isolated from *P. falciparum* trophozoites/early schizonts.** Occurrences of DRM-associated proteins in each functional class are reported as a histogram.

(PF3D7_1347200); the rhoptry-associated antigen RAMA (PF3D7_0707300); and three proteins exported beyond the parasite plasma membrane: the PV-localized protease SERA5 (PF3D7_0207600), a member of a family of putative papain-like proteases SERA, with a role in parasite egress; the PVM-resident ETRAMP5 (PF3D7_0532100), which belongs to the early transcribed membrane protein family; and a member of the Pfmc-2-TM family localized to the MCs (PF3D7_0222100).

Expression Profile of Genes Encoding DRM Components—RNA sequencing data from synchronous asexual and sexual *P. falciparum* blood stages (available in PlasmoDB) were analyzed to assess the expression profile of genes encoding DRM-associated proteins (Fig. 2). Normalized RNA values of each gene at the different time points of infection were grouped in six clusters of co-regulated genes by the self-organizing tree clustering algorithm. Genes activated/up-regulated at the trophic stages (clusters 1–3) encode the majority of DRM-associated proteins involved in transport, metabolic pathways, and protein translation, wheras the products of genes grouped in clusters 3 and 4, activated/up-regulated in late trophozoites and schizonts, include the majority of proteins related to invasion. A small subset of genes transcribed at a higher level in rings and/or early throphozoites (clusters 1 and 2) includes the three translocon components detected in this study: PTEX150 (PF3D7_1436300), HSP101 (PF3D7_1116800), and Exp2 (PF3D7_1471100).

Predicted Localization Signals in DRM-associated Proteins—About 60% of the DRM-associated proteins are predicted to contain a signal peptide (SP) and/or a transmembrane domain (TM). Within this subset, the relative abundance of proteins containing an SP or an SP plus a TM significantly differs from that calculated for the entire trophozoite proteome, whereas proteins containing TM regions display similar abundance (Fig. 3). Six SP-containing proteins are GPI-anchored, and three identified proteins (PF3D7_0222100, PF3D7_0721100, and PF3D7_1407800) have been predicted to contain a plasmodium export element motif (26, 27) that directs the export of parasite-encoded proteins beyond the PVM via the translocon machinery (2). These data support a role of DRMs in the sorting/trafficking of parasite proteins to intra- or extracellular membrane compartments.

Validation of Trophozoite DRM Proteome—To validate our proteomic data, we selected and characterized six proteins (Table II) containing a predicted localization signal or having a role in protein folding/trafficking. Recombinant proteins, expressed as GST fusions, were purified and used to prepare mouse immune sera. Their specificity was verified by Western blot analysis on total cell lysate prepared from *P. falciparum*-infected and non-infected RBCs (supplemental Fig. S1). The immune sera tested reacted exclusively with the iRBCs and recognized protein bands of the expected size, with the exception of the immune serum specific for PfN201. In that case, antibodies reacted strongly with a 250-kDa polypeptide and faintly with two additional protein bands, one at the expected size of around 100 kDa and the other at 150 kDa, suggesting that PfN201 may form homo-/heterodimers not completely disrupted in SDS-PAGE. Consistently, PfN201 (also known as Pf113) was detected associated with high molecular mass complexes (>400 kDa) in DRMs of *P. falciparum* schizonts (16, 17).

To investigate the stage-specific expression of the selected proteins, we probed time-course samples from a highly synchronous *P. falciparum* infection with the characterized immune sera (Fig. 4). Specific protein bands were mainly detected in trophozoites/early schizonts (Fig. 4*A*) and in late schizonts (Fig. 4*B*), with the exception of the Pfmc-2-TM family members, which were absent in mature schizonts. The abundance of cognate transcripts is reported in Fig. 4*C*.

In order to verify the association of the selected proteins with DRMs, purified trophozoites were treated with Triton-X100 at 4 °C after erythrocyte lysis and cell extracts were subjected to discontinuous sucrose gradient centrifugation. The effectiveness of the gradient separation was verified by probing the collected fractions for the presence of the erythrocyte Flotillin 1 (28) and Band 3 (13), which partition into DRM rafts, or the skeletal protein Spectrin, excluded from this compartment (Fig. 5). All *Plasmodium* proteins analyzed were detected in floating low-density fractions but displayed different buoyancy profiles; PFJ130, PFB985, and the 250-kDa protein band, which includes PFN201, partition into DRMs with a buoyant density similar to that of the erythrocyte raft markers (fractions 3–5), whereas PFL1070c, PFK55, and PFK351 partition into DRMs with a higher buoyant density (fractions 5 and 6).

Lipid Composition of DRMs Contained in P. falciparum iRBCs—The different buoyancy of parasite proteins associ-

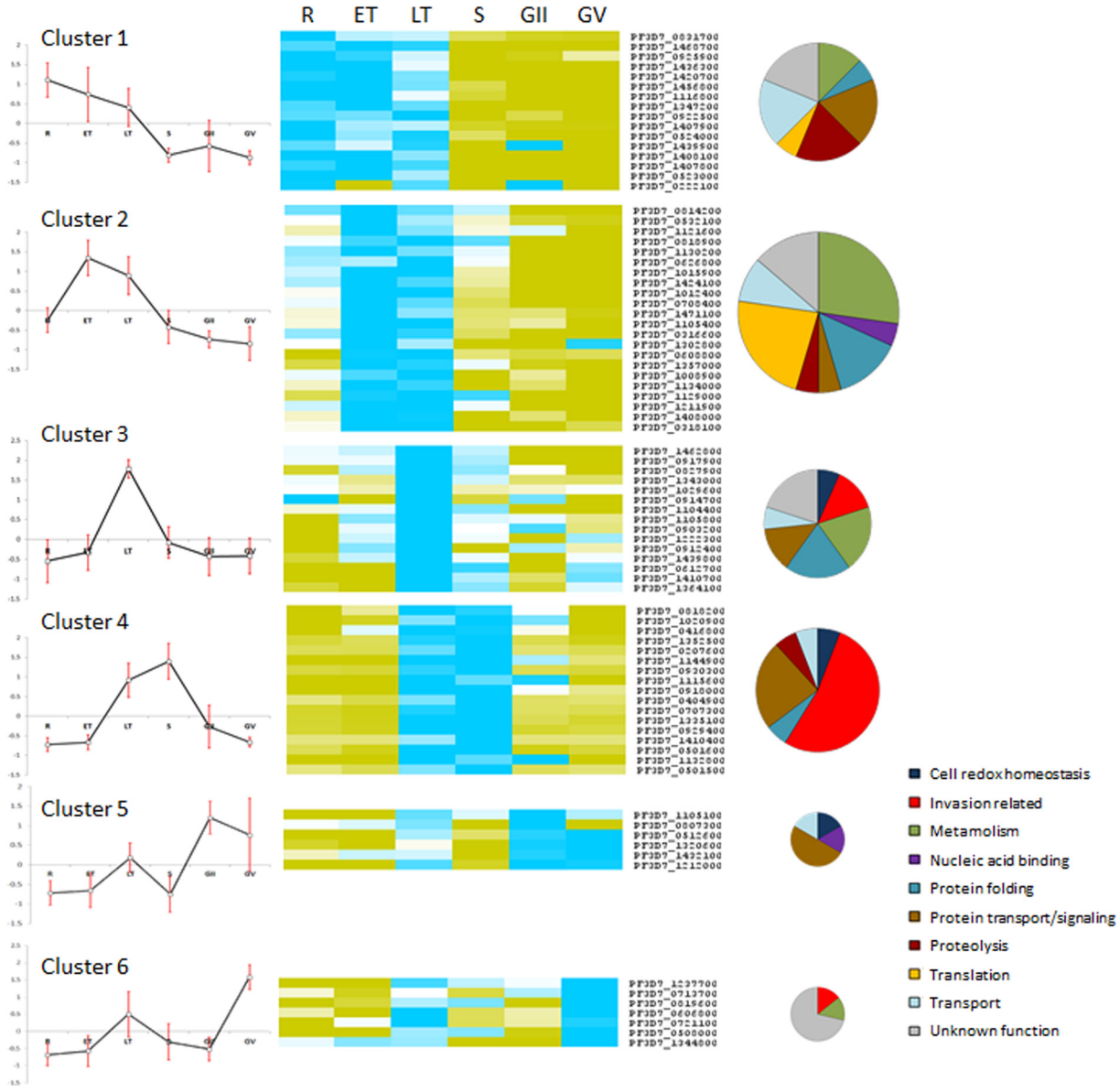

FIG. 2. **Expression profiles of genes encoding DRM-associated proteins.** Data from RNA sequencing of *P. falciparum* blood stages (20), available in PlasmoDB, were used to determine the expression profiles of genes encoding DRM-associated proteins at different time points of parasite development: ring (R), early trophozoite (ET), late trophozoite (LT), schizont (S), and early (GII) and late (GV) gametocytes. Blue and yellow boxes correspond to positive and negative values, respectively, and zero is shown as a white box. Six clusters were identified by the self-organizing tree clustering algorithm. For each cluster, a centroid profile is shown (left) in which red bars represent the standard deviations at each time point. Pie charts represent the functional classification of proteins in each cluster.

ated with DRMs may reflect heterogeneity in the lipid compositions of membrane microdomains they are embedded in. To verify this, we analyzed lipid components of total parasite extract and low-density gradient fractions 2–6, containing the majority of floating DRMs. As expected, the relative abundance of lipid species in pooled DRM fractions differed from that of total parasite extract (Fig. 6*A*). Notably, when cholesterol and phospholipids (phosphatidylcholine, phosphatidylethanolamine) and sphingomyelin were measured in each DRM fraction, we observed that individual lipid species are differently represented along the gradient (Fig. 6*B*).

DRMs Localize to Various Membrane Compartments of P. falciparum iRBCs—Subcellular localization of the selected proteins was investigated via indirect immunofluorescence assay on paraformaldehyde-fixed trophozoite-infected RBCs (Fig. 7). PfJ130 contains a predicted signal peptide and a hydrophobic stretch of amino acids close to its C terminus. This conserved protein of unknown function also was identified in the DRM proteome of mixed blood stages of the rodent malaria parasite *P. berghei* (Table I). Specific antibodies identified a confined dotted labeling within the parasite cytoplasm. PfN201, characterized by an N-terminal signal peptide fol-

lowed by a cysteine-rich region, co-localized with the PVM resident protein EXP1. PfB985 belongs to the MC-resident 2TM family, composed of 13 members, which exhibit more than 90% identity (29). Raised antibodies, expected to react with all the expressed 2TM proteins, confirmed the subcellular localization of these molecules. PfK351, an Hsp70 chaperone homolog, is mainly localized to parasite mitochondrion, as indicated via overlay with mitotracker labeling. PfL1070, an endoplasmin homolog, contains a predicted SP and an endoplasmic reticulum (ER) retention signal SDEL at the C terminus. Co-immunofluorescence with the ER-resident marker PfBiP confirmed the ER localization of this protein. PfK55, a conserved hypothetical protein with unknown function, contains an SP and an ER retention signal (KDEL), strongly suggesting ER targeting. However, due to the poor reactivity of the specific immune serum in the indirect immunofluorescence assay, the exact subcellular localization of this protein remained elusive.

Overall, these results indicated that membranes of *P. falciparum*–infected erythrocytes contain distinct types of DRMs, most likely characterized by specific protein and lipid contents. These assemblies are present in membrane structures exported beyond the *P. falciparum* plasma membrane (PVM, MCs), as well as intracellular compartments/organelles such as the mitochondrion and the ER.

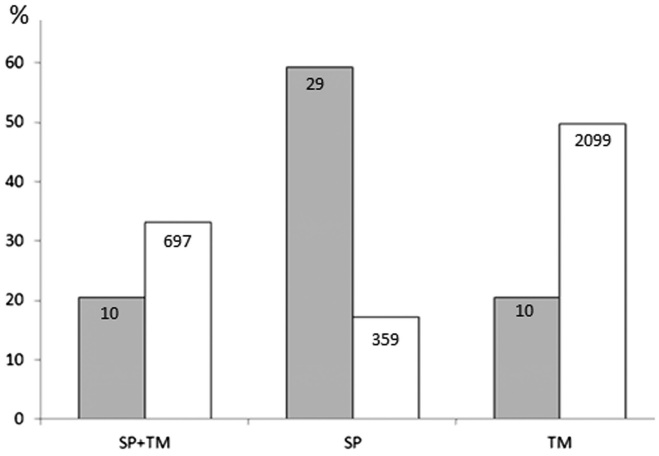

FIG. 3. **Relative abundance of proteins containing localization signals.** The percentages of DRM-associated proteins with a signal peptide (SP) and/or a transmembrane domain (TM) (gray bars) are compared with those of the entire trophozoite proteome (white bars). A chi-squared test was performed to evaluate the significance of the observed differences ($p < 10^{-10}$).

DISCUSSION

DRM Rafts in Malaria Parasite Infection and Pathogenesis—The existence and properties of DRMs in human erythrocytes have been described recently (13, 30, 31), and their involvement in invasion by malaria parasite is amply documented. The cholesterol-depleting agent methyl-β-cyclodextrin abolishes parasite entry into erythrocytes (32). A similar effect was also observed when erythrocytes were treated with lidocaine, a local anesthetic that affects DRM-raft organization, without any alteration of the membrane cholesterol content (33). Moreover, major merozoite structural proteins involved in the early stages of invasion reside in cholesterol-rich membranes (16, 34–39). During parasite entry, extensive remodeling of the erythrocyte DRM rafts occurs (13, 40) with selective recruitment of host DRM-associated proteins into the newly formed PVM, most likely induced by proteinaceous parasite ligands present in the invasion-associated apical organelles (reviewed in Ref. 41).

These studies indicated that DRM-based interactions of both host and parasite origin are essential for the invasion process. However, the subcellular localization, organization, and dynamics of DRMs during parasite development inside the host erythrocyte were poorly explored. A limited number of parasite proteins were characterized as DRM-associated in *P. falciparum* trophic stages, and the majority of them localize to the PVM. These include the PVM-resident proteins EXP1 and EXP2, the rhoptry components, Pf-stomatin and RhopH2 (34), translocated across the parasitophorous vacuole upon invasion, and, importantly, the recently characterized export machinery (2).

In this study, we performed two independent proteomic analyses of DRM rafts isolated from *P. falciparum*–infected erythrocytes at the late trophozoite/early schizont stage of development. The first experiment (A) was carried out using a long chromatographic peptide separation and a linear ion-trap

TABLE II

Selected DRM-associated proteins. Six DRM-associated proteins containing a signal peptide (SP) or a transmembrane domain (TM) or having a role in protein folding/trafficking were selected for the production of specific mouse immune sera. Protein regions expressed in bacteria are indicated

Gene ID	Parasite protein	SP	TM	Expected molecular weight (kDa)	Expressed region (amino acids)	Annotation
PF3D7_1104400	PfK55	+	−	49	98–321	Conserved protein, unknown function (ER retention signal KDEL)
PF3D7_1013300	PfJ130	+	1C-term	75	39–186	Conserved protein, unknown function
PF3D7_1134000	PfK351	−	−	73	195–496	Heat shock protein hsp70 homologue
PF3D7_1222300	PfL1070	+	−	95	27–416	Endoplasmin homolog (ER retention signal SDEL)
PF3D7_0222100	PfB985	+	2C-term	27	73–176	Pfmc-2TM family member 2.2 (PEXEL/HCT motif)
PF3D7_1420700	PfN201	+	1C-term	112	44–257	Surface protein, Pf113

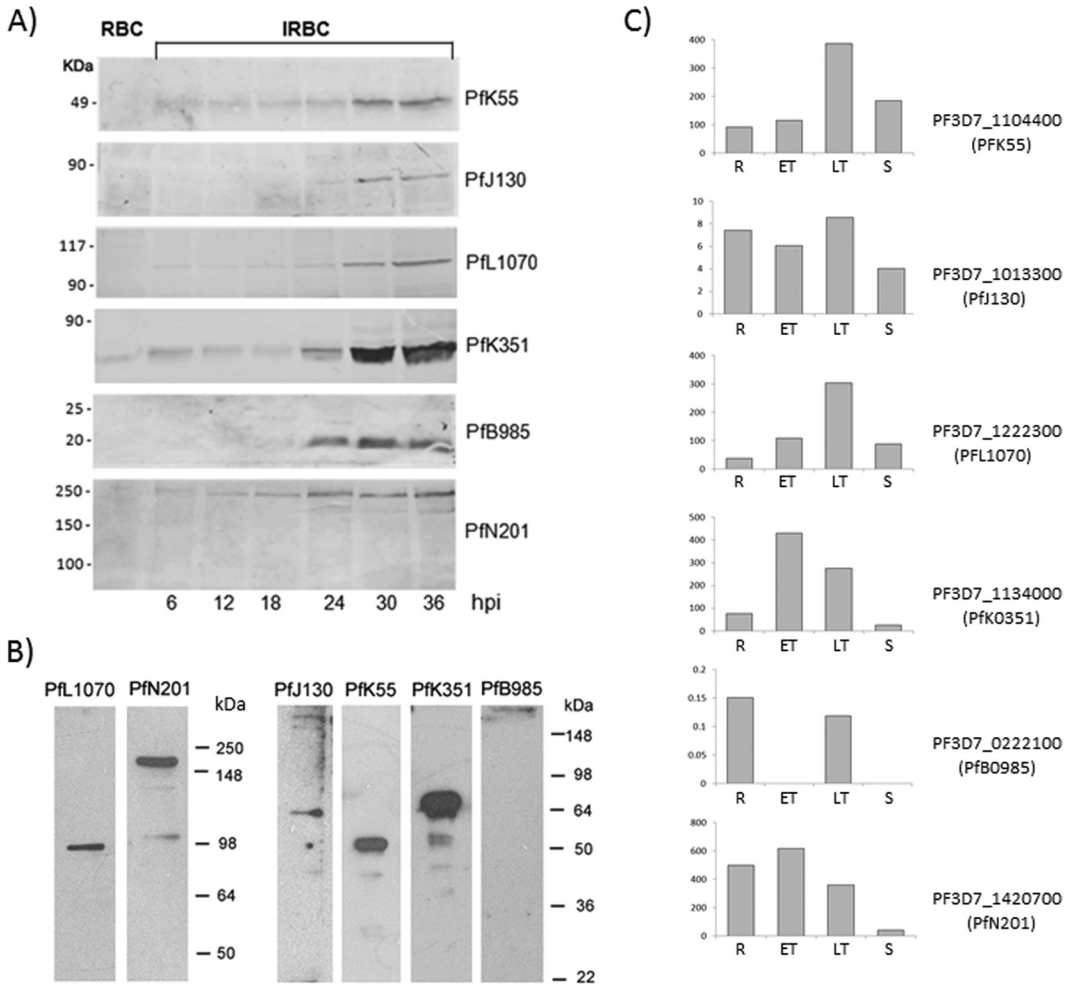

FIG. 4. **Expression profiles of six proteins identified in trophozoite/early schizont DRM proteome.** Samples from a synchronous *P. falciparum* culture were taken at different hours post infection (hpi) and probed with immune sera raised against PFJ130, PFN201, PFB985c, PFL1070c, PFK55, and PFK351 proteins (*A*). Noninfected erythrocyte extract (RBC) was loaded as a negative control. Specific signals are detected exclusively in the infected erythrocytes (iRBC), mainly at the trophozoite and early schizont stages (24–36 hpi). All proteins except PFB985c were also detected in late schizonts (*B*). RNA sequencing data (20) were exploited to determine the relative abundance of the specific transcripts in rings (R), early trophozoites (ET), late trophozoites (LT), and schizonts (S) shown in *C*.

mass spectrometer and led to the identification of 158 parasite proteins, whereas the second experiment (B), based on electrophoretic separation of the proteins and employing a hybrid quadrupole TOF mass spectrometer, identified 93 parasite proteins. The difference in the number of detected proteins is not surprising, mainly because the two experiments were run on mass spectrometers with different peptide ionization efficiencies and scan rates (42). Moreover, the different separation methods employed (long gradient and PAGE) may explain in part the observed discrepancy. To be confident, we considered only the 84 proteins identified in both experiments for further analyses. These molecules mainly fall into four broad functional categories: metabolism, protein transport/signaling, folding, and proteolysis. We detected an abundance of chaperones and RAB-GTPases, as well as components of the machinery that mediates the translocation of parasite proteins across the PVM (2). This strongly suggests that DRMs at the trophozoite stage recruit molecules implicated in the establishment of new pathways of protein sorting and trafficking within the iRBC.

Consistent with the idea that DRM association varies depending on the parasite's developmental stage, we detected four plasmepsins, PM I, PM II, PM III (or HAP), and PM IV, involved in catabolism of the host hemoglobin (25), a process characteristic of *Plasmodium* trophic stages. These aspartic proteases are type II integral membrane proteins routed to a lysosomal compartment, the food vacuole. Deletion of each of the individual genes did not affect parasite viability, indicating substantial functional redundancy (43). These proteases are trafficked to the food vacuole via the parasite plasma membrane, where they incorporate as inactive proenzymes into forming cytostomes, which deliver hemoglobin to the food vacuole (44). Once at the food vacuole, PMs are activated and released from the membrane by means of proteolytic cleav-

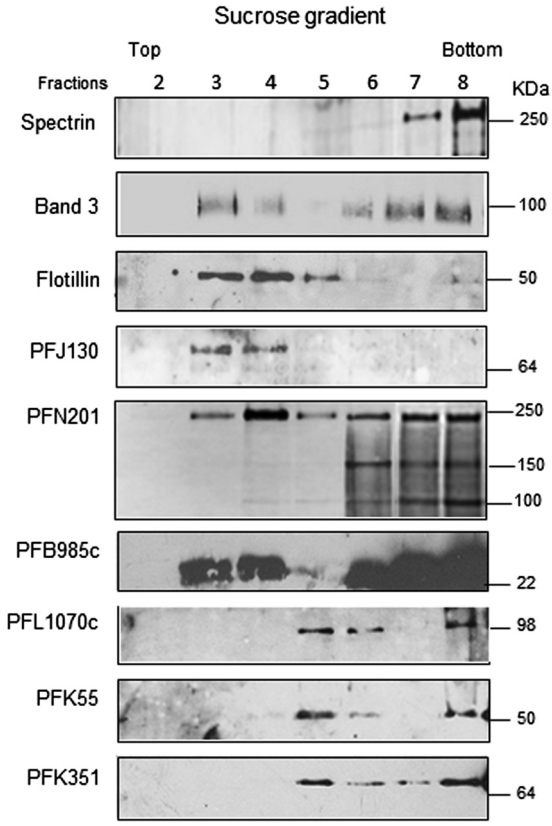

FIG. 5. **DRM association of the selected proteins.** Trophozoite-enriched iRBCs were purified from a synchronous *P. falciparum* culture and treated with cold Triton-X100 after erythrocyte lysis. Cell extract was subjected to discontinuous sucrose gradient centrifugation. Proteins associated with triton-insoluble membranes float to the low-density fractions (2–6) of the gradient, whereas proteins associated with triton-soluble membranes remain mainly confined to the loading zone (high-density fractions). Equal volumes of fractions 2–8, collected from the top to the bottom of the gradient, were probed with antibodies raised against Flotillin 1 and Band3 (associated with erythrocyte DRMs), the erythrocyte skeletal protein Spectrin (excluded from this compartment), and the *P. falciparum* proteins PFJ130, PFN201, PFB985c, PFL1070c, PFK55, and PFK351.

age (45). The detection of PMs in DRM fractions suggests that specialized raft-like membrane microdomains may be implicated in this internalization process.

DRMs Are Present in Various Membrane Compartments of P. falciparum–infected Erythrocytes—To validate our proteomic data and to gain insights into DRM-dependent functions, we prepared immune sera against six putative DRM-associated proteins that had not been previously characterized. Candidates were selected for the presence of predicted localization signals or for their potential role in protein folding/trafficking. Sucrose gradient fractions probed with the specific immune sera indicated that all the selected proteins partitioned into DRMs, although five out of six were also detected in Triton-soluble high-density fractions, suggesting that their incorporation in cholesterol-rich microdomains is dynamic. Immunolocalization studies showed that the selected proteins are targeted to various subcellular compartments of the iRBC, including internal organelles. PfK55 and PfL1070 contain a predicted SP and an ER retention signal. Co-localization with the ER resident protein PfBiP was clearly shown for PfL1070. PfJ130, predicted to contain an SP, was detected in confined dot-like structures inside the parasite, whereas PfK351 localized to the mitochondrion. The existence of different populations of DRMs routed to internal membrane compartments of *P. falciparum* has not yet been documented, although increasing evidence suggests that in other organisms raft-like regions reside in internal organelles and not only in the plasma membrane. For example, two ER proteins, members of the family of prohibitin domain-containing proteins, referred to as erlin-1 and -2, were identified in the detergent-insoluble low-density fractions of different cell types (46). A subdomain of the ER, the mitochondria-associated membrane, was shown to mediate cross-talk between the ER and mitochondria. This domain regulates important processes such as Ca^{2+} signaling and protein folding (47). DRM-associated proteins at the mitochondria–mitochondria-associated membrane interface most likely coordinate these events (47). Raft-like membrane microdomains were also identified in mitochondria and shown to be implicated in mitochondrial fission processes (48).

In this study, we identified two novel membrane proteins associated with DRMs and exported beyond the parasite plasma membrane, PfN201 (PF3D7_1420700), which localizes to the PVM, and PfB985 (PF3D7_0222100), targeted to the MCs. PfN201, also known as surface protein Pf113, contains a predicted SP followed by a cystein-rich stretch and a putative GPI-anchor sequence. It was previously identified in the DRM proteome of *P. falciparum* late schizonts (16) and shown to be present in high molecular mass complexes (>400 kDa) (17), even though subcellular localization and DRM association of this protein were not proved. PfB985 is a member of the PfMC-2TM family. These proteins, localized to the MCs (29), were also identified in a proteomic study of *P. falciparum*–infected erythrocyte ghosts (4). Here we showed, for the first time, the presence of raft-like structures in MC membranes. This supports previous observations that the assembly and translocation of virulence factors PfEMP1 (22) and PIRs (18) to the host cell surface involve insertion at cholesterol-rich microdomains.

Lipid Composition of DRM Microdomains in the Trophozoite iRBCs—Although a variety of cell functions take place in DRM rafts, where proteins and lipids interact intimately (for a review, see Ref. 49), few studies have analyzed the diversity of the lipid composition of these membrane microdomains (50). In this study, specific antibodies revealed a diverse flotation capacity of DRM-associated proteins upon sucrose gradient centrifugation, suggesting that they are embedded in different lipid contexts. This was confirmed by the analysis of major lipid classes present in low-density gradient fractions 2–6. We observed, in fact, that the relative abundance of cholesterol

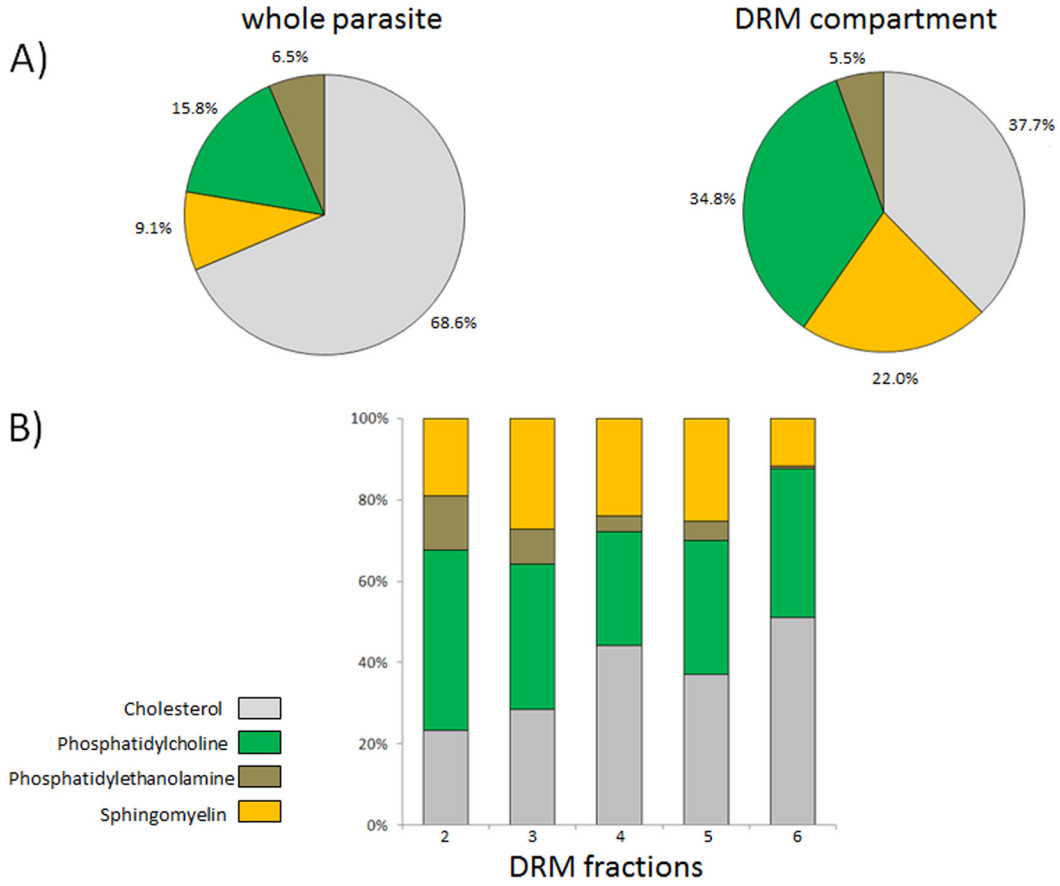

FIG. 6. **Lipid components of DRM fractions.** Relative abundance (expressed as a percentage) of lipids from pooled DRM fractions (2–6) or unfractionated trophozoites after erythrocyte lysis is shown in the pie charts (*A*). The lipid content of each DRM fraction is shown in *B*.

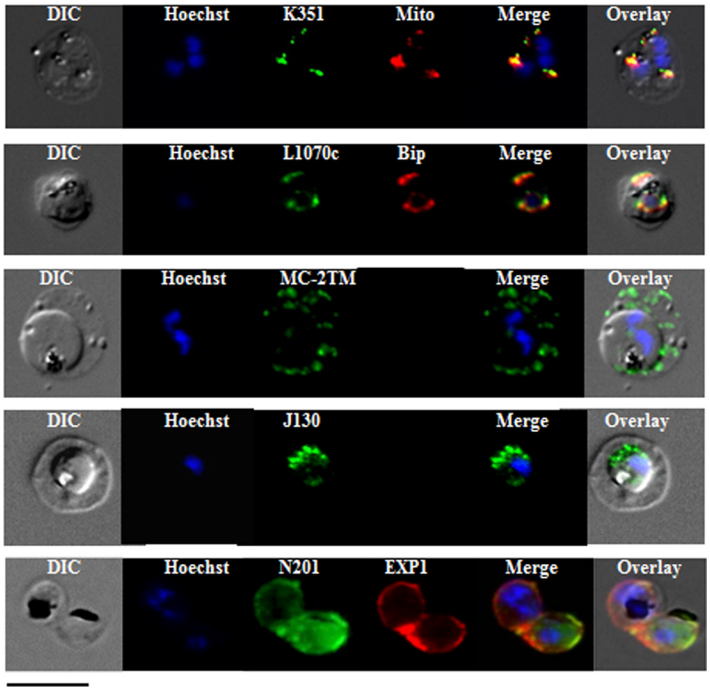

FIG. 7. **Subcellular localization of *P. falciparum* DRM-associated proteins.** Immunofluorescence studies were performed on paraformaldehyde-fixed *P. falciparum* trophozoite-infected RBCs using mouse immune sera raised against the DRM-associated proteins PFJ130, PFN201, PFB985, PFL1070c, and PFK351. Immune sera specific for PfBip and PfEXP1 were used for co-labeling, as indicated. Mitochondria labeling was performed with the MitoTracker® probe. Parasite nuclei were stained with Hoechst 33342. Microscopic observations were made on an apotome-equipped Axio Imager 2 (Carl Ziess, Jena) with a 100× apochromat objective and differential interference contrast (DIC). The DIC merged and overlay images are presented. Bar size: 5 μm.

and phospholipids, phosphatidylethanolamine, phosphatidylcholine, and sphingomyelin differs in each DRM-containing fraction. The existence of raft-like domains with distinct properties has been previously proposed for late endosomes, which contain cholesterol-rich microdomains both in their limiting membrane and in intraluminal vesicles (51). It was also shown that the fractionation patterns for two *falciparum* detergent-resistant rhoptry proteins differ, suggesting that multiple DRM populations exist within this organelle (52).

In conclusion, this study provides insights into the protein composition and subcellular localization of DRM rafts isolated from *P. falciparum* trophozoites/early schizonts. We showed that these assemblies are heterogeneous in subcellular localization, lipid composition, and, most likely, set of associated proteins. We expect that further investigation of the complexity and dynamical flexibility of DRMs during the different developmental stages of the *Plasmodium* parasite will provide important knowledge for the design of novel intervention strategies.

* The research leading to these results has received funding from the European Community's Seventh Framework Programme (FP7/2007–2013) under Grant Agreement No. 242095, from the Italian FLAGSHIP "InterOmics" project (PB.P05) funded by MIUR and coordinated by the CNR, and from MalParTraining, an FP6-funded Marie Curie Action under Contract No. MEST-CT-2005-020492.

[S] This article contains supplemental material.

¶¶ To whom correspondence should be addressed: Dipartimento di Malattie Infettive, Parassitarie ed Immunomediate, Istituto Superiore di Sanità, Viale Regina Elena 299, 00161, Rome, Italy, Tel.: 39-064990-2868, Fax: 39-064990-2226, E-mail: marta.ponzi@iss.it.

§ These authors contributed to this work equally.

¶ Current affiliation: Nanyang Technological University, 60 Nanyang Dr., Singapore 637551, Singapore.

** Current affiliation: Laboratory Medicine, Department of Laboratories, Bambino Gesù Children's Hospital, IRCCS, Piazza Sant'Onofrio 4, 00165, Rome, Italy.

REFERENCES

1. Maier, A. G., Cooke, B. M., Cowman, A. F., and Tilley, L. (2009) Malaria parasite proteins that remodel the host erythrocyte. *Nat. Rev. Microbiol* **5,** 341–354
2. de Koning-Ward, T. F., Gilson, P. R., Boddey, J. A., Rug, M., Smith, B. J., Papenfuss, A. T., Sanders, P. R., Lundie, R. J., Maier, A. G., Cowman, A. F., and Crabb, B. S. (2009) A newly discovered protein export machine in malaria parasites. *Nature* **7249,** 945–949
3. Taraschi, T. F., Trelka, D., Martinez, S., Schneider, T., and O'Donnell, M. E. (2001) Vesicle-mediated trafficking of parasite proteins to the host cell cytosol and erythrocyte surface membrane in *Plasmodium falciparum* infected erythrocytes. *Int. J. Parasitol.* **12,** 1381–1391
4. Vincensini, L., Richert, S., Blisnick, T., Van Dorsselaer, A., Leize-Wagner, E., Rabilloud, T., and Braun Breton, C. (2005) Proteomic analysis identifies novel proteins of the Maurer's clefts, a secretory compartment delivering *Plasmodium falciparum* proteins to the surface of its host cell. *Mol. Cell. Proteomics* **4,** 582–593
5. Wickham, M. E., Rug, M., Ralph, S. A., Klonis, N., McFadden, G. I., Tilley, L., and Cowman, A. F. (2001) Trafficking and assembly of the cytoadherence complex in *Plasmodium falciparum*-infected human erythrocytes. *EMBO J.* **20,** 5636–5649
6. Hanssen, E., Carlton, P., Deed, S., Klonis, N., Sedat, J., DeRisi, J., and Tilley, L. (2010) Whole cell imaging reveals novel modular features of the exomembrane system of the malaria parasite, *Plasmodium falciparum. Int. J. Parasitol.* **40,** 123–134
7. Shevchenko, A., and Simons, K. (2010) Lipidomics: coming to grips with lipid diversity. *Nat. Rev. Mol. Cell Biol.* **11,** 593–598
8. Goldston, A. M., Powell, R. R., and Temesvari, L. A. (2012) Sink or swim: lipid rafts in parasite pathogenesis. *Trends Parasitol.* **28,** 417–426
9. Vieira, F. S., Corrêa, G., Einicker-Lamas, M., and Coutinho-Silva, R. (2010) Host-cell lipid rafts: a safe door for micro-organisms? *Biol. Cell* **102,** 391–407
10. Simons, K., and Gerl, M. J. (2010) Revitalizing membrane rafts: new tools and insights. *Nat. Rev. Mol. Cell Biol.* **11,** 688–699
11. Brown, D. A., and London, E. (2000) Structure and function of sphingolipid- and cholesterol-rich membrane rafts. *J. Biol. Chem.* **275,** 17221–17224
12. Mañes, S., del Real, G., and Martínez, A. C. (2003) Pathogens: raft hijackers. *Nat. Rev. Immunol.* **3,** 557–568
13. Murphy, S. C., Samuel, B. U., Harrison, T., Speicher, K. D., Speicher, D. W., Reid, M. E., Prohaska, R. Low, P. S., Tanner, M. J., Mohandas, N., and Haldar, K. (2004) Erythrocyte detergent-resistant membrane proteins: their characterization and selective uptake during malarial infection. *Blood* **103,** 1920–1928
14. Murphy, S. C., Fernandez-Pol, S., Chung, P. H., Prasanna Murthy, S. N., Milne, S. B., Salomao, M., Brown, H. A., Lomasney, J. W., Mohandas, N., and Haldar, K. (2007) Cytoplasmic remodeling of erythrocyte raft lipids during infection by the human malaria parasite *Plasmodium falciparum. Blood* **110,** 2132–2139
15. Labaied, M., Jayabalasingham, B., Bano, N., Cha, S. J., Sandoval, J., Guan, G., and Coppens, I. (2011) *Plasmodium* salvages cholesterol internalized by LDL and synthesized de novo in the liver. *Cell. Microbiol.* **13,** 569–586
16. Sanders, P. R., Gilson, P. R., Cantin, G. T., Greenbaum, D. C., Nebl, T., Carucci, D. J., McConville, M. J., Schofield, L., Hodder, A. N., Yates, J. R., 3rd, and Crabb, B. S. (2005) Distinct protein classes including novel merozoite surface antigens in raft-like membranes of *Plasmodium falciparum. J. Biol. Chem.* **280,** 40169–40176
17. Sanders, P. R., Cantin, G. T., Greenbaum, D. C., Gilson, P. R., Nebl, T., Moritz, R. L., Yates, J. R., 3rd, Hodder, A. N., and Crabb, B. S. (2007) Identification of protein complexes in detergent-resistant membranes of *Plasmodium falciparum* schizonts. *Mol. Biochem. Parasitol.* **154,** 148–157
18. Di Girolamo, F., Raggi, C., Birago, C., Pizzi, E., Lalle, M., Picci, L., Pace, T., Bachi, A., de Jong, J., Janse, C. J., Waters, A. P., Sargiacomo, M., and Ponzi, M. (2008) Plasmodium lipid rafts contain proteins implicated in vesicular trafficking and signalling as well as members of the PIR superfamily, potentially implicated in host immune system interactions. *Proteomics* **8,** 2500–2513
19. Trager, W., and Jensen, J. (1976) Human malaria parasites in continuous culture. *Science* **193,** 673–675
20. López-Barragán, M. J., Lemieux, J., Quiñones, M., Williamson, K. C., Molina-Cruz, A., Cui, K., Barillas-Mury, C., Zhao, K., and Su, X. Z. (2011) Directional gene expression and antisense transcripts in sexual and asexual stages of Plasmodium falciparum. *BMC Genomics* **12,** 587
21. Sargeant, T. J., Marti, M., Caler, E., Carlton, J. M., Simpson, K., Speed, T. P., and Cowman, A. F. (2006) Lineage-specific expansion of proteins exported to erythrocytes in malaria parasites. *Genome Biol.* **7,** R12
22. Folch, J., Lees, M., and Sloane Stanley, G. H. (1957) A simple method for the isolation and purification of total lipides from animal tissues. *J. Biol. Chem.* **226,** 497–509
23. Frankland, S., Adisa, A., Horrocks, P., Taraschi, T. F., Schneider, T., Elliott, S. R., Rogerson, S. J., Knuepfer, E., Cowman, A. F., Newbold, C. I., and Tilley, L. (2006) Delivery of the malaria virulence protein PfEMP1 to the erythrocyte surface requires cholesterol-rich domains. *Eukaryot. Cell* **5,** 849–860
24. van Dijk, M. R., van Schaijk, B. C., Khan, S. M., van Dooren, M. W., Ramesar, J., Kaczanowski, S., van Gemert, G. J., Kroeze, H., Stunnenberg, H. G., Eling, W. M., Sauerwein, R. W., Waters, A. P., and Janse, C. J. (2010) Three members of the 6-cys protein family of *Plasmodium* play a role in gamete fertility. *PLoS Pathog.* **6,** e1000853
25. Banerjee, R., Liu, J., Beatty, W., Pelosof, L., Klemba, M., and Goldberg, D. E. (2002) Four plasmepsins are active in the *Plasmodium falciparum* food vacuole, including a protease with an active-site histidine. *Proc. Natl. Acad. Sci. U.S.A.* **99,** 990–995
26. Hiller, N. L., Bhattacharjee, S., van Ooij, C., Liolios, K., Harrison, T., Lopez-Estrano, C., and Haldar, K. (2004) Host-targeting signal in virulence proteins reveals a secretome in malarial infection. *Science* **5703,**

1934–1937
27. Marti, M., Good, R. T., Rug, M., Knuepfer, E., and Cowman, A. F. (2004) Targeting malaria virulence and remodeling proteins to the host erythrocyte. *Science* **5703,** 1930–1933
28. Salzer, U., and Prohaska, R. (2001) Stomatin, flotillin-1, and flotillin-2 are major integral proteins of erythrocyte lipid rafts. *Blood* **97,** 1141–1143
29. Sam-Yellowe, T. Y., Florens, L., Johnson, J. R., Wang, T., Drazba, J. A., Le Roch, K. G., Zhou, Y., Batalov, S., Carucci, D. J., Winzeler, E. A., and Yates, J. R., 3rd. (2004) A *Plasmodium* gene family encoding Maurer's cleft membrane proteins: structural properties and expression profiling. *Genome Res.* **14,** 1052–1059
30. Salzer, U., Hinterdorfer, P., Hunger, U., Borken, C., and Prohaska, R. (2002) Ca(++)-dependent vesicle release from erythrocytes involves stomatin-specific lipid rafts, synexin (annexin VII), and sorcin. *Blood* **99,** 2569–2577
31. Ciana, A., Balduini, C., and Minetti, G. (2005) Detergent-resistant membranes in human erythrocytes and their connection to the membrane-skeleton. *J. Biosci.* **30,** 317–328
32. Samuel, B. U., Mohandas, N., Harrison, T., McManus, H., Rosse, W., Reid, M., and Haldar, K. (2001) The role of cholesterol and glycosylphosphatidylinositol-anchored proteins of erythrocyte rafts in regulating raft protein content and malarial infection. *J. Biol. Chem.* **276,** 29319–29329
33. Koshino, I., and Takakuwa, Y. (2009) Disruption of lipid rafts by lidocaine inhibits erythrocyte invasion by Plasmodium falciparum. *Exp. Parasitol.* **123,** 381–383
34. Hiller, N. L., Akompong, T., Morrow, J. S., Holder, A. A., and Haldar, K. (2003) Identification of a stomatin orthologue in vacuoles induced in human erythrocytes by malaria parasites: a role for microbial raft proteins in apicomplexan vacuole biogenesis. *J. Biol. Chem.* **278,** 48413–48421
35. Wang, L., Mohandas, N., Thomas, A., and Coppel, R. L. (2003) Detection of detergent-resistant membranes in asexual blood-stage parasites of *Plasmodium falciparum. Mol. Biochem. Parasitol.* **130,** 149–153
36. Hoessli, D. C., Poincelet, M., Gupta, R., Ilangumaran, S., and Nasir-ud-Din (2003) Plasmodium falciparum merozoite surface protein 1. *Eur. J. Biochem.* **270,** 366–375
37. Topolska, A. E., Lidgett, A., Truman, D., Fujioka, H., and Coppel, R. L. (2004) Characterization of a membrane-associated rhoptry protein of *Plasmodium falciparum. J. Biol. Chem.* **279,** 4648–4656
38. Black, C. G., Wang, L., Topolska, A. E., Finkelstein, D. I., Horne, M. K., Thomas, A. W., Mohandas, N., and Coppel, R. L. (2004) Merozoite surface proteins 4 and 5 of *Plasmodium knowlesi* have differing cellular localisation and association with lipid rafts. *Mol. Biochem. Parasitol.* **138,** 153–158
39. Proellocks, N. I., Kovacevic, S., Ferguson, D. J., Kats, L. M., Morahan, B. J., Black, C. G., Waller, K. L., and Coppel, R. L. (2007) Plasmodium falciparum Pf34, a novel GPI-anchored rhoptry protein found in detergent-resistant microdomains. *Int. J. Parasitol.* **37,** 1233–1241
40. Lauer, S., VanWye, J., Harrison, T., McManus, H., Samuel, B. U., Hiller, N. L., Mohandas, N., and Haldar, K. (2000) Vacuolar uptake of host components, and a role for cholesterol and sphingomyelin in malarial infection. *EMBO J.* **19,** 3556–3564
41. Murphy, S. C., Hiller, N. L., Harrison, T., Lomasney, J. W., Mohandas, N., and Haldar K. (2006) Lipid rafts and malaria parasite infection of erythrocytes. *Mol. Membr. Biol.* **23,** 81–88
42. Elias, J. E., Haas, W., Faherty, B. K., and Gygi, S. P. (2005) Comparative evaluation of mass spectrometry platforms used in large-scale proteomics investigations. *Nat. Methods* **2,** 667–675
43. Liu, J., Gluzman, I. Y., Drew, M. E., and Goldberg, D. E. (2005) The role of *Plasmodium falciparum* food vacuole plasmepsins. *J. Biol. Chem.* **280,** 1432–1437
44. Klemba, M., Beatty, W., Gluzman, I., and Goldberg, D. E. (2004) Trafficking of plasmepsin II to the food vacuole of the malaria parasite *Plasmodium falciparum. J. Cell Biol.* **164,** 47–56
45. Drew, M. E., Banerjee, R., Uffman, E. W., Gilbertson, S., Rosenthal, P. J., and Goldberg, D. E. (2008) Plasmodium food vacuole plasmepsins are activated by falcipains. *J. Biol. Chem.* **283,** 12870–12876
46. Browman, D. T., Resek, M. E., Zajchowski, L. D., and Robbins, S. M. (2006) Erlin-1 and erlin-2 are novel members of the prohibitin family of proteins that define lipid-raft-like domains of the ER. *J. Cell Sci.* **119,** 3149–3160
47. Hayashi, T., and Fujimoto, M. (2010) Detergent-resistant microdomains determine the localization of sigma-1 receptors to the endoplasmic reticulum-mitochondria junction. *Mol. Pharmacol.* **77,** 517–528
48. Ciarlo, L., Manganelli, V., Garofalo, T., Matarrese, P., Tinari, A., Misasi, R., Malorni, W., and Sorice, M. (2010) Association of fission proteins with mitochondrial raft-like domains. *Cell Death Differ.* **17,** 1047–1058
49. van Meer, G., Voelker, D. R., and Feigenson, G. W. (2008) Membrane lipids: where they are and how they behave. *Nat. Rev. Mol. Cell Biol.* **9,** 112–124
50. Martin, R. E., Elliott, M. H., Brush, R. S., and Anderson, R. E. (2005) Detailed characterization of the lipid composition of detergent-resistant membranes from photoreceptor rod outer segment membranes. *Invest. Ophthalmol. Vis. Sci.* **46,** 1147–1154
51. Sobo, K., Chevallier, J., Parton, R. G., Gruenberg, J., and van der Goot, F. G. (2007) Diversity of raft-like domains in late endosomes. *PLoS One* **2(4),** e391
52. Proellocks, N. I., Kovacevic, S., Ferguson, D. J., Kats, L. M., Morahan, B. J., Black, C. G., Waller, K. L., and Coppel, R. L. (2007) Plasmodium falciparum Pf34, a novel GPI-anchored rhoptry protein found in detergent-resistant microdomains. *Int. J. Parasitol.* **37,** 1233–1241